International Journal of Pharmaceutics 433 (2012) 157–164

Contents lists available at SciVerse ScienceDirect

International Journal of Pharmaceutics

journal homepage: www.elsevier.com/locate/ijpharm

Pharmaceutical Nanotechnology

Studies on the preparation, characterization and pharmacokinetics of Amoitone B nanocrystals

Leilei Hao[a,1], Xiaoyong Wang[b,1], Dianrui Zhang[a,*], Qingyan Xu[b], Siyang Song[b], Feihu Wang[a], Caiyun Li[a], Hejian Guo[a], Yue Liu[a], Dandan Zheng[a], Qiang Zhang[c]

[a] Department of Pharmaceutics, College of Pharmacy, Shandong University, 44 Wenhua Xilu, Jinan 250012, PR China
[b] State Key Laboratory of Stress Cellular Biology, School of Life Sciences, Xiamen University, Xiamen, Fujian 361005, PR China
[c] State Key Laboratory of Natural and Biomimetic Drugs, School of Pharmaceutical Sciences, Peking University, 38 Bei Xueyuan Road, Beijing 100083, PR China

ARTICLE INFO

Article history:
Received 4 April 2012
Received in revised form 27 April 2012
Accepted 3 May 2012
Available online 11 May 2012

Keywords:
Amoitone B
Nanocrystals
Microfluidization method
In vitro dissolution
Pharmacokinetics

ABSTRACT

Amoitone B, as a new derivative of cytosporone B, has been proved to be a natural agonist for Nur77. It exhibits remarkable anticancer activity in vivo and has the potential to be a therapeutic agent for cancer treatment. However, the poor solubility and dissolution rate result in low therapeutic index for injection and low bioavailability for oral administration, therefore limiting its application. In order to magnify the clinical use of Amoitone B, nanocrystal was selected as an application technology to solve the above problems. In this study, the optimized Amoitone B nanocrystals with small and uniform particle size were successfully prepared by microfluidization method and investigated by morphology, size distribution, and zeta potential. The differential scanning calorimetry (DSC) and X-ray diffraction (XRD) confirmed there was no crystalline state changed in the size reduction process. For Amoitone B nanocrystals, an accelerated dissolution velocity and increased saturation solubility were achieved in vitro and a markedly different pharmacokinetic property in vivo was exhibited with retarded clearance and magnified AUC compared with Amoitone B solution. These results implied that developing Amoitone B as nanocrystals is a promising choice for intravenous delivery and further application for cancer therapy.

1. Introduction

Nur77, also known as TR3 or NGFI-B, is a unique transcription factor belonging to the orphan nuclear receptor superfamily (Maruyama et al., 1998) and no physiologic ligand for Nur77 has been identified until now. Nur77 is also an immediate-early gene induced by serum, growth factors and receptor engagement, participating in a variety of biological processes including regulating proliferation, differentiation and apoptosis (Li et al., 2006; Winoto and Littman, 2002). Studies have shown that Nur77 is often overexpressed in a variety of cancer cells, such as lung (Kolluri et al., 2003), pancreatic (Yoon et al., 2011), colon (Cho et al., 2007), ovarian (Sibayama-Imazu et al., 2008) and stomach (Wu et al., 2002). In these cancer cells, Nur77 functions in the nucleus as an oncogenic survival factor, but becomes a potent killer when certain death stimuli induce its migration to mitochondria, where Nur77 interacts with Bcl-2 and induces its conformational change, resulting in conversion of Bcl-2 from a protector to a killer that triggers cytochrome *c* release and apoptosis (Lin et al., 2004; Moll et al., 2006; Thompson and Winoto, 2008). Furthermore, Nur77 also plays an important role in stimulating glucose production (Pei et al., 2006) and reducing lipid loading and inflammatory responses in atherogenesis (Bonta et al., 2007). So the unique property of Nur77 makes it an attractive molecular target for developing new therapeutics for the treatment of cancer and related diseases.

The octaketide cytosporone B (Csn-B), a natural Nur77 agonist isolated from Dothiorella sp. HTF3 (Brady et al., 2000), has the ability to directly bind to and activate Nur77, leading to induction of apoptosis via translocation of Nur77 to the mitochondria (Zhan et al., 2008). Amoitone B (*n*-amyl-2-[3,5-dihydroxy-2-(1-nonanoyl) phenyl] acetate) whose structure is shown in Fig. 1, is one of series of novel Csn-B analogs synthesized (Liu et al., 2010). It possesses similar functions to Csn-B but with enhanced Nur77-binding and activating properties, exhibiting remarkable anticancer activity in both cell culture and xenograft tumors (Liu et al., 2010). As the most effective derivative, Amoitone B that bound to Nur77 tightly not only stimulated its transactivation activity but also initiated mitochondrial apoptosis by means of novel cross-talk between Nur77 and brain and reproductive organ-expressed protein (BRE), an anti-apoptotic protein which specifically downregulates death receptor-mediated apoptosis (Chan et al., 2008; Li et al., 2004; Liu et al., 2010). Thus, Amoitone B, a novel Nur77 agonist, has the potential to be used as a therapeutic agent for cancer treatment.

* Corresponding author. Tel.: +86 531 88382015; fax: +86 531 88382015.
E-mail address: zhangdianrui2006@163.com (D. Zhang).
[1] These authors contributed equally to this paper.

0378-5173/$ – see front matter © 2012 Elsevier B.V. All rights reserved.
http://dx.doi.org/10.1016/j.ijpharm.2012.05.002

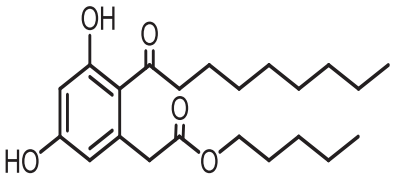

Fig. 1. Chemical structure of Amoitone B.

Nowadays, more attentions are paid to the effects of Amoitone B, nevertheless, the water-insolubility and poor bioavailability limit its application.

Recently, various nanonization strategies have emerged to improve the dissolution rates and solubility of insoluble drugs, for example, nanoemulsions, polymeric nanomicelles, nanostructured lipid carriers and nanocrystals (Chen et al., 2011; Zhang et al., 2011). Wherein, nanocrystal technology which can be applied to all poorly soluble drugs is the most simple and practical approach because all these drugs could be directly disintegrated into nanosizing particles. As we know, drugs in nanosuspensions exist in two forms: crystalline state and amorphous state; when the drug particles exist in the form of crystalline state, they are called nanocrystals (Liu et al., 2012a; Thassu et al., 2007). Nanocrystals, a carrier-free colloidal drug delivery system, consist essentially of pure drug crystals and a minimum amount of surface active agent required for stabilization, and have been applied to tackle the formulation issue of poorly soluble drugs (Keck and Muller, 2006). With particle size in nanometer range and enormous particle surface area, nanocrystals can significantly increase the dissolution velocity and saturation solubility of insoluble drugs, therefore improving their bioavailability and biological effects. An important advantage of nanocrystals is that when applied in oral administration, the increased adhesion to the gastrointestinal mucosa and the prolonged contact time will enhance absorption of drugs via the gastrointestinal tract (Kayser, 2001; Mou et al., 2011). Apart from that, due to its sufficiently small size and safe compositions, nanocrystals can be injected intravenously to overcome the dissolution problem of insoluble drugs and adverse toxicity caused by the solvent mixture or co-solvents used in the traditional injection and 100% bioavailability can be obtained (Gao et al., 2008a; Muller and Keck, 2004). Moreover, nanocrystals can passively target infection sites or organs by following phagocytosis of the reticuloendothelial system (Gao et al., 2008b) and may also show active targeting features by modification of the crude drug or stabilizers using appropriate materials with target activity (Liu et al., 2012a).

At present, a variety of production techniques have been applied to produce drug nanocrystals, such as precipitation (Chen et al., 2008, 2004), Wet milling (Cerdeira et al., 2010), high pressure homogenization (Wang et al., 2010) and microfluidization (Verma et al., 2009a), as well as combined methods such as emulsion–diffusion followed by homogenization (Dolenc et al., 2009) and the solvent displacement coupled with ultrasonication (Latha et al., 2009). Among these techniques, microfluidization, a newly developed method which can generate a better homogeneous effect due to the higher pressure provided, is the most convenient and easiest to scale up for industrial production. The operation process is as following: the coarse suspensions consisting of drug, stabilizers, and dispersion medium are made to pass through the specially designed interaction chambers at a high velocity, then the suspensions are broken up into two streams with direction changed when a series of forces come into being, such as shear force, turbulence, impaction, and cavitation forces (Tsai et al., 2009; Verma et al., 2009a). The forces above and the attrition between the particles and against the chamber walls lead to particle size reduction (Verma et al., 2009b).

In this paper, the Amoitone B nanocrystals were prepared by microfluidization method to overcome its water insolubility and poor dissolution behavior, and the optimum formula was obtained through the screening of different stabilizers and process parameters. For Amoitone B nanocrystals, the physicochemical properties were evaluated including morphology, size distribution, zeta potential and crystalline state. In addition, in vitro dissolution behavior and in vivo pharmacokinetics were studied in detail. To date, this is the first research report on the pharmaceutical preparation for Amoitone B, thus having important significances for further research and application.

2. Materials and methods

2.1. Materials

Amoitone B was synthesized by Xiamen University and was kindly donated by Professor Shen. Poloxamer 188 (F68) was purchased from Sigma (USA). Lecithin for injection administration was obtained from Shanghai Taiwei Medicine Co. Ltd., China. Hydroxypropyl methyl cellulose (HPMC) was provided by Zhengzhou Tianying Chemical Co. Ltd. Mannitol (analytical grade) was generously supplied by Tianjin Guangcheng chemical agent Co. Ltd., China. Methanol (HPLC grade) was purchased from Tianjin Siyou Fine Chemicals Co. Ltd., China. All the other chemicals and reagents were of chromatographic or analytical grade.

2.2. Preparation of Amoitone B nanocrystals

Nanocrystal suspensions were prepared by microfluidization technology. Briefly, 0.1 g of Amoitone B powders were dispersed in 30 mL of aqueous solution containing 0.1 g lecithin and 0.1 g F68 under ultrasound stirring for 15 min, then the suspensions were pre-milled by an Ultra-Turrax® T25 (IKA, Germany) at 20,000 rpm for 10 min. The suspensions were further processed through a microfluidizer model M-110P (Microfluidics, USA), firstly performing 3 cycles at 500 bar and 3 cycles at 1000 bar as the pre-milling to protect the interaction chambers from blocking and then 15 cycles at 1800 bar to obtain Amoitone B nanosuspensions. For long-term stability, based on the preliminary experimental results, the prepared Amoitone B nanosuspensions with 5% (W/V) mannitol added as cryoprotectant were rapidly cooled down at −80 °C Ultra-low Temperature Freezer (DW-86L, Haier, China) for 24 h and then freeze-dried for 48 h at −50 °C with a FD-1000 freeze dryer (EYELA, Japan). Following all the operations mentioned above, the final Amoitone B nanocrystal powders we called NC-Am for short were obtained and they would be used for all experiments in the following.

The Amoitone B physical mixture sample with the same compositions was also prepared as control, but instead of microfluidization operation, it was only stirred under ultrasound. This sample was also transformed into freeze-dried powders using mannitol as cryoprotectant.

2.3. Characterization of Amoitone B nanocrystals

2.3.1. Particle size and zeta potential analysis

The particle size and zeta potential value of the Amoitone B nanocrystal suspensions were determined by the Delsa™ Nano C Particle Analyzer (Beckman Coulter, Inc.). The freeze-dried powders were redispersed with water to obtain a proper scattering intensity before measurement. All measurements were made in triplicate.

2.3.2. Morphology observation by transmission electron microscope (TEM)

The transmission electron microscopy (TEM) (H-7000, Hitachi, Japan) was used to evaluate the morphology of Amoitone B nanosuspensions and its freeze-dried powders. The freeze-dried powders were dissolved and diluted with water to obtain a moderate concentration, and then a drop of the samples was placed on a 200-mesh copper grid, negatively stained with 2% phosphotungstic acid for 30 s, dried at room temperature and then observed by TEM.

2.3.3. Crystalline state

Before and after particle size reduction, differential scanning calorimetry (DSC) and X-ray diffraction (XRD) analysis were conducted to confirm whether the initial crystalline state was changed or not. The thermal properties of Amoitone B, the excipients, their physical mixture and the freeze-dried Amoitone B nanocrystal powders (NC-Am) were investigated with a DSC-41 apparatus (Shimadzu, Japan). The samples, approximately 3–4 mg based on the capability of heat absorption, were placed in a hermetically closed aluminum pan and α-Al_2O_3 was used as a reference. The heating rate of the scanning calorimeter was 10 °C min^{-1} from 25 to 500 °C.

The crystalline forms of the systems, including Amoitone B, the excipients, as well as the physical mixture and freeze-dried powders (NC-Am), were investigated by a D/max R-B X-ray diffractometer (Rigaku, Japan). XRD diffractograms were recorded by Cu Kα radiation with a wavelength of 1.5405 Å at 40 kV and 100 mA. Samples were scanned at a step size of 0.02°over a 2θ range of 3–50°.

2.4. Solubility determination

In order to assess whether the saturation solubility of Amoitone B was enhanced after nanosizing, the solubility experiments were conducted with a magnetic stirrer (RCT Basic, IKA, Staufen, Germany). Excess pure Amoitone B and the prepared nanocrystal powders NC-Am, as well as the physical mixture were dispersed in 10 mL 0.1% (W/V, g mL^{-1}) SDS aqueous solution and 0.05% (V/V) Tween 80 aqueous solution, respectively. The temperature and stirring rate were set at 37 ± 0.5 °C and 100 rpm, respectively. After shaken for 72 h, 1 mL samples were withdrawn and centrifuged at 14,000 rpm for 10 min with Zonkia HC-2062 high speed centrifuge (Anhui USTC Zonkia Scientific Instruments Co., Ltd.), then the supernatants were filtered using 0.22 μm microporous membrane filters before HPLC analysis. The experiment was made in triplicate.

2.5. Dissolution experiments

For any route of administration, the bioavailability of nanocrystals ultimately depends on the dissolution of drugs, so the dissolution behavior of Amoitone B nanocrystal powders (NC-Am) should be systematically evaluated. Accurately weighed samples containing approximately 2 mg Amoitone B were suspended in 200 mL dissolution medium and were stirred (100 rpm) on a magnetic stirrer (RCT Basic, IKA, Staufen, Germany) at 37 ± 0.5 °C for 120 min. For the purpose of investigating the dissolution behaviors of Amoitone B in different media and maintaining sink conditions, 0.1% SDS aqueous solution and 0.05% Tween 80 aqueous solution were selected as the dissolution media. At predetermined intervals, 0.5 mL aliquot was withdrawn and 0.5 mL blank medium was immediately added back into the vessels to maintain the constant volume. To compare the extent that the dissolution rate was increased, the dissolution behaviors of three groups including Amoitone B, physical mixture and NC-Am were all studied. The withdrawn samples were filtered and analyzed by HPLC method. Each sample was analyzed in triplicate.

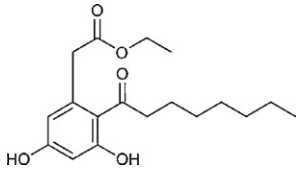

Fig. 2. Chemical structure of Amoitone A.

2.6. HPLC analysis

The concentration of the drug in the dissolution tests was determined by an Agilent 1260 HPLC system (Agilent, USA) with a ZORBAX Eclipse XDB-C_{18} column (4.6 mm × 150 mm, 5 μm). The mobile phase is methanol–water mixture (90:10, V/V). The flow rate was 0.5 mL min^{-1} and the detection wavelength was set to 300 nm.

2.7. Animals

New Zealand white rabbits (2.5 ± 0.2 kg), supplied by the Experimental Animal Center of Shandong University (Jinan, China), were used for pharmacokinetic study. At first, the animals were acclimatized at a temperature of 25 ± 2 °C under natural light/dark conditions for 1 week and were fed with food and water ad libitum. Prior to the experiment, the animals were kept fasting overnight. All experimental procedures abided by the ethics and regulations of animal experiments of Pharmaceutical Sciences, Shandong University, China.

2.8. Pharmacokinetics study

Eight New Zealand white rabbits were randomly and equally divided into two groups. Two formulations, Amoitone B solution and Amoitone B nanocrystals (NC-Am), were administered to the two groups, respectively, at an 8.0 mg kg^{-1} dose level via the left auricular vein after dilation with 75% ethanol solution. The nanocrystals were dispersed in 5% glucose solution, and Amoitone B solution was prepared as a control by dissolving Amoitone B with mixture solvent of PEG400/ethanol/1,2-propylene glycol/physiologic saline (3/1/1/5, V/V/V/V). Blood samples were drawn via the right auricular vein using heparinized tubes at predetermined time points (for Amoitone B solution at 0.08, 0.17, 0.33, 0.5, 1, 2, 4, 6 h after i.v., and for NC-Am at 0.08, 0.17, 0.33, 0.5, 1, 2, 4, 6, 8, 10 h after i.v.). Blood samples were centrifuged at 14,000 rpm for 10 min, and then the serum was separated and stored at −20 °C until analysis.

2.9. Serum sample analysis

100 μL of serum were extracted and homogenized with sodium hydroxide solution (20 μL, 1.0 mol L^{-1}) on a vortex mixer (GENIE-2, Scientific industries Inc., America) for 1 min, placed in room temperature to react for 5 min. An internal standard Amoitone A (Fig. 2, Zhan et al., 2008) methanol solution (10 μL, 10 μg mL^{-1}) was added and vortex-mixed for 1 min, then 300 μL of acetic ether was added and rigorously mixed for 3 min. After centrifuging at 14,000 rpm for 5 min, the organic layer was transferred to another tube and the extraction process was repeated once more. Afterwards, hydrochloric acid solution (20 μL, 1.0 mol L^{-1}) was added into the combined organic phases, vortex-mixed for 1 min and centrifuged at 14, 000 rpm for 5 min, then the supernatant was evaporated under a light stream of nitrogen at 37 °C. The residue was dissolved in 100 μL of acetonitrile, and finally 20 μL was injected for HPLC analysis. The blood concentration was calculated

Table 1
Composition of Amoitone B nanocrystal suspensions.

Formulation	Amoitone B (g)	F68 (g)	Lecithin (g)	HPMC (g)	Water (mL)
1	0.1	0.2	0.0	0.0	30
2	0.1	0.0	0.2	0.0	30
3	0.1	0.0	0.0	0.2	30
4	0.1	0.05	0.1	0.0	30
5	0.1	0.1	0.05	0.0	30
6	0.1	0.1	0.1	0.0	30
7	0.1	0.0	0.1	0.1	30
8	0.1	0.1	0.0	0.1	30
9	0.1	0.1	0.05	0.05	30
10	0.1	0.05	0.1	0.05	30

by comparison with the linear regression equation derived from the standard curve.

The plasma samples were analyzed by an Agilent 1260 HPLC analysis system (Agilent, USA) with a ZORBAX Eclipse XDB-C_{18} column (4.6 mm × 150 mm, 5 μm). The mobile phase consisted of methanol–water (82:18, V/V) at a flow rate of 0.6 mL min^{-1}. The detection wavelength was 300 nm and the column temperature was set to 30 °C.

2.10. Statistics

Statistical analysis was performed using Student's *t*-test with $P < 0.05$ indicating significant difference. Pharmacokinetic parameters were obtained using drug and statistics (DAS) version 2.0 software (Mathematical Pharmacology Professional Committee of China, Shanghai, China).

3. Results and discussion

3.1. Screening of formulations with different types and concentrations of stabilizers

As we know, a kind of surfactant or polymer is necessary for the stabilization of nanocrystals which had increased surface area after nanosizing process. So it is of critical importance to screen the types and concentrations of stabilizers for obtaining the optimal formulation composition with long-term storage stability. In the preliminary experiments, F68, lecithin and HPMC were used as stabilizers to screen the optimal prescription for Amoitone B with the particle size, zeta potential and storage stability taken into consideration. In this study, ten formulations as shown in Table 1 were investigated by the microfluidization method. After the homogenization process, compared with other prescriptions, formula 6, 9, 10 were all found with much smaller and more uniform particle size between 200 nm and 300 nm, and with suitable zeta potential of about −20 mV to −30 mV. Moreover, after stored at 4 °C for 1 week, the nanosuspensions of formula 6, 9, 10 showed a better short-term stability and redispersibility without significant changes of the particle size and zeta potential. However, in order to avoid the possible side effects such as anaphylactic response and vascular irritability which may be caused by surfactants, it is more secure to reduce the types and amounts of the stabilizers used to some extent. Thus, formula 6 was selected as the finally optimized preparation prescription with the particle size and zeta potential of about 261.3 nm and −21.52 mV, respectively. Besides, for long-term storage stability and convenient transportation, the nanosuspensions should be transformed into dry powders by freeze-drying technology.

3.2. Screening of the parameters of preparation

Figs. 3 and 4 showed the influences of homogenization pressure and cycle numbers on the particle size distribution of Amoitone B nanosuspensions. The higher pressure and increased cycles mean that the energy conducted on drug particles is higher, so the crystals that cannot be cracked at lower pressure can be broken down. During the microfluidization process, the investigated homogenization pressure were set to 200 bar, 500 bar, 800 bar, 1000 bar, 1500 bar, 1800 bar with the same cycle number of 10 and the cycle numbers were set to 2, 4, 8, 12, 15, 18 at the same pressure of 1800 bar. Judging from Figs. 3 and 4, as the homogenization pressure and cycle numbers increased step by step, the mean particle size and polydispersity index (PI) decreased gradually, suggesting more and more uniform and stable systems were obtained. Considering the above results and preliminary experiments, the Amoitone B nanosuspensions were prepared in the optimized procedure by firstly using the pressure of 500 bar and 1000 bar for 3 cycles, respectively, and then the high pressure of 1800 bar was applied for 15 cycles. The final particle size was about 256.3 nm with PI of 0.206.

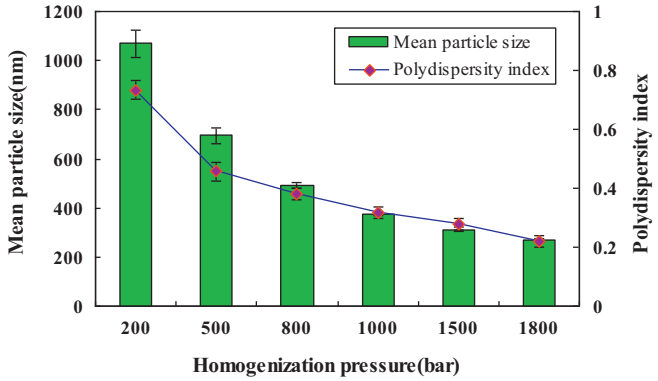

Fig. 3. Influence of different homogenization pressures on the particle size and polydispersity index of Amoitone B nanosuspensions. Data were expressed as mean ± S.D., $n = 3$.

3.3. Zeta potential

The zeta potential of the nanosuspensions allows predictions about the storage stability of colloidal dispersions. In general, the zeta potential value at least ±30 mV can ensure the physically stability of nanosuspensions when using ionic surfactants for electric repulsion; however, a zeta potential about ±20 mV can also signify long-term stability of the system when nonionic surfactants were applied for steric hindrance. In addition, the type of stabilizers was a key variable that had prominent effect on the mean zeta potential value. In our test, formula 6 which used F68 and lecithin as stabilizers was an electrostatic and steric system, and the zeta potentials of its nanosuspensions and freeze-dried powders were

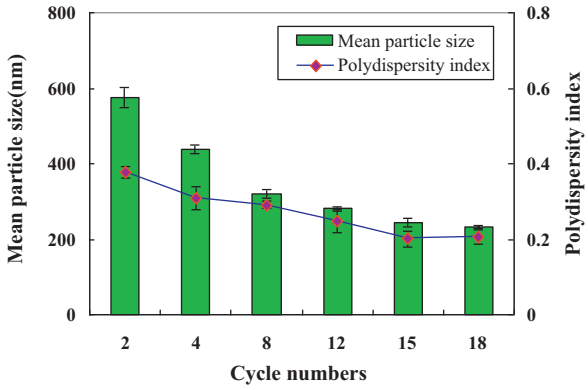

Fig. 4. Influence of different cycle numbers on the particle size and polydispersity index of Amoitone B nanosuspensions. Data were expressed as mean ± S.D., $n = 3$.

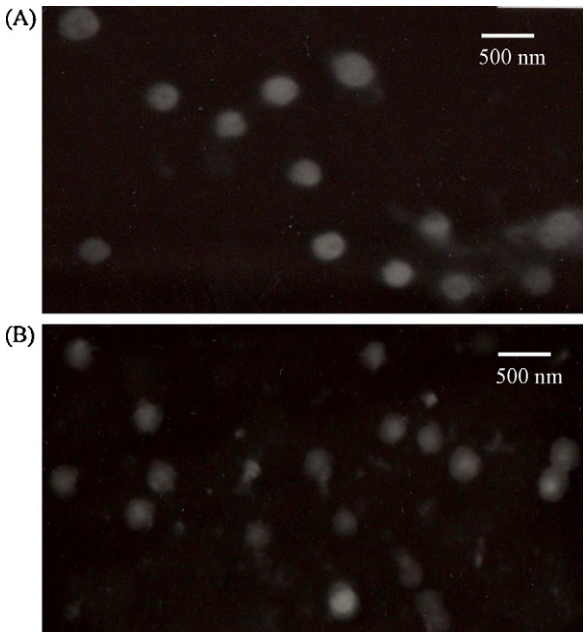

Fig. 5. Transmission electron micrographs of the Amoitone B nanosuspensions (A) and freeze-dried powders (NC-Am) after dispersal in water (B).

−21.52 ± 0.82 mV and −24.05 ± 0.59 mV, respectively. As the particle aggregation is less likely to occur if possessing enough zeta potential, formula 6 was expected to be a stable preparation.

3.4. Morphology observation by TEM

The morphology of the optimized Amoitone B nanocrystals prepared by the microfluidization method was analyzed by TEM. The morphological characterizations of the Amoitone B nanosuspensions and freeze-dried powders (NC-Am) were shown in Fig. 5. It displayed that they were in spherical shape and non-adherent among each other. After 15 cycles at 1800 bar, a homogeneous system was observed with small and uniform particle size of about 256.3 nm for the Amoitone B nanosuspensions and about 275.4 nm for NC-Am. Owing to the uniformity of this system, there is little tendency of aggregation or adhesion among particles, suggesting that the formula with a good stability was obtained by microfluidization technology.

3.5. Crystalline state

The assessment of the crystalline state contributes to understanding the polymorphic changes that drugs might undergo during the nanosizing and freeze-drying operations. Furthermore, the crystalline state is also a key indicator as it relates to the saturation solubility and physical stability of the nanosuspension systems. The DSC and XRD analysis were carried out to evaluate the crystalline state of the Amoitone B nanocrystals (NC-Am) and investigate the interaction among different components during the preparation process. As shown in Fig. 6, the DSC characteristic peaks of pure Amoitone B (106.4 °C, A), Pluronic F68 (57.3 °C, B), and mannitol (168.3 °C, 349.1 °C, D) could be found in the DSC curves of NC-Am (F) as well as the physical mixture (E), meaning that the initial crystalline forms of the drug and its excipients were reserved. However, the peak of Amoitone B had a slightly migration in NC-Am (F), which might be explained by the interaction with the excipients of F68, lecithin and mannitol. In addition, the heat capacity, heating rate and the amount of substance may influence the peak position and intensity, leading to the deviation.

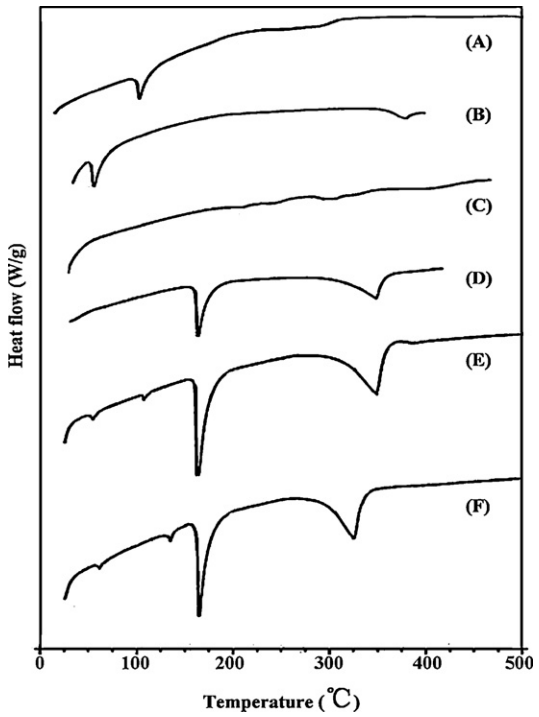

Fig. 6. DSC thermograms of Amoitone B (A), F68 (B), lecithin (C), mannitol (D), physical mixture (E), and NC-Am (F).

The XRD analysis was shown in Fig. 7, the characteristic peaks of Amoitone B (at 2θ of 6.20°, 21.38° and 22.56°, A) could be found in the profiles of Amoitone B nanocrystal powders (F) and the physical mixture (E). This result further confirmed that the microfluidization process had no influence on the Amoitone B crystalline state. As we know, the amorphous form can generally enhance the dissolution rate and bioavailability of drugs due to its high-energy (Fakes et al., 2009). According to that principle and with both the DSC and the XRD analysis considered, we can conclude that the enhancement of dissolution rate of Amoitone B may be due to the reduction of particle size or the influence of surfactants rather than the appearance of amorphous form. Moreover, compared with the amorphous form, the maintenance of initial crystalline state was beneficial to a long-term stability.

3.6. Solubility studies

Table 2 showed the saturation solubility of pure Amoitone B, the physical mixture, and Amoitone B nanocrystals in dissolution media of 0.1% SDS aqueous solution and 0.05% Tween 80 aqueous solution, respectively. According to Table 2, compared with pure Amoitone B, the solubility of the physical mixture was increased due to the surfactants F68 and lecithin, however, their solubilization effects were finite most often. Hence, the noticeable increased saturation solubility of Amoitone B in the formulation of nanocrystals was mainly attributed to the decreased particle size and increased surface area. The results can be explained by the Ostwald–Freundlich equation which demonstrates that the

Table 2
Saturation solubility of Amoitone B, physical mixture, and Amoitone B nanocrystals (NC-Am). Data were represented with mean ± S.D., $n = 3$ ($\mu g\,mL^{-1}$).

Saturation solubility	Amoitone B	Physical mixture	NC-Am
0.1% SDS solution	26.94 ± 0.58	151.22 ± 1.62	405.53 ± 1.73
0.05% Tween 80 solution	72.11 ± 1.23	110.33 ± 1.76	388.20 ± 2.07

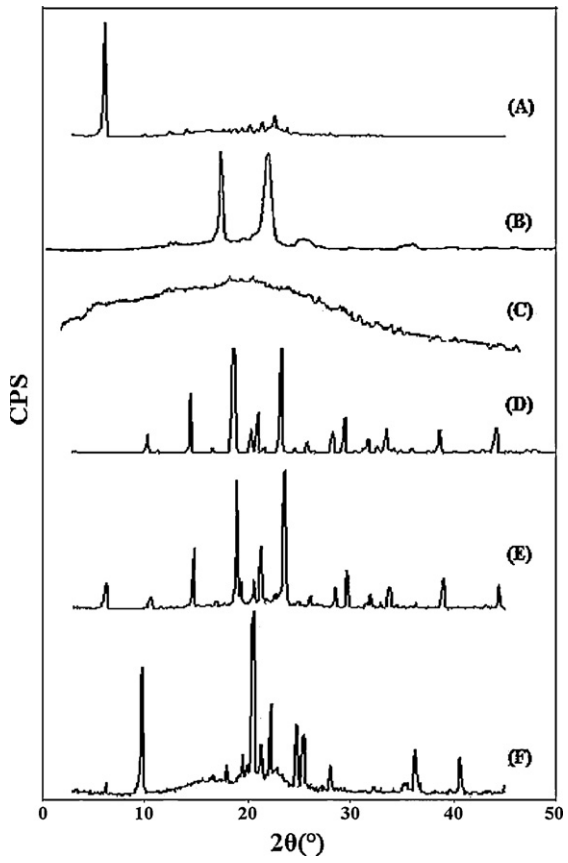

Fig. 7. X-ray diffractograms for Amoitone B (A), F68 (B), lecithin (C), mannitol (D), physical mixture (E), and NC-Am (F).

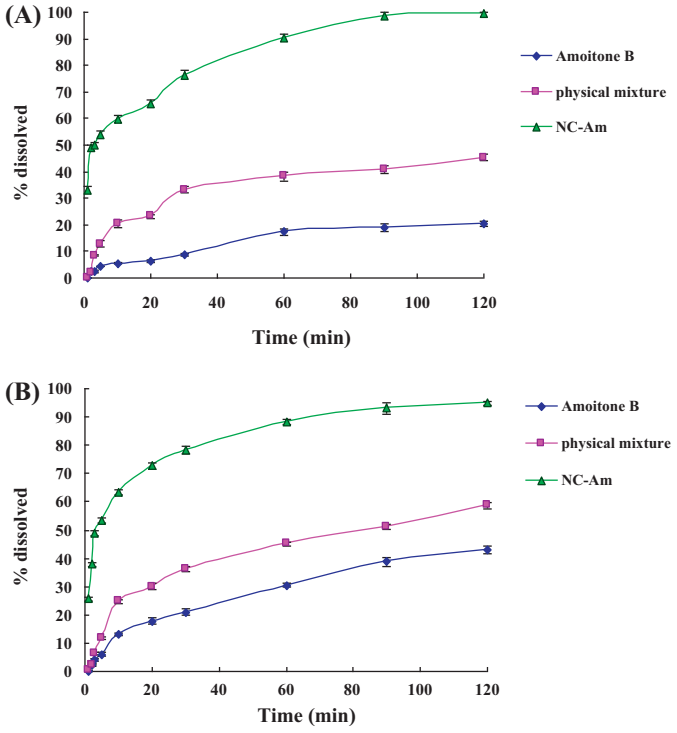

Fig. 8. Dissolution profiles of pure Amoitone B, physical mixture and the optimized Amoitone B nanocrystals (NC-Am) in 0.1% SDS solution (A) and in 0.05% Tween 80 solution (B).

saturation solubility of the drug increases with reduction of particle size (Böhm and Müller, 1999).

3.7. Dissolution studies

The dissolution behaviors in vitro were performed for the purpose of ascertaining whether the goal of improving the dissolution rate of Amoitone B was achieved. In order to satisfy the sink conditions, 0.1% SDS aqueous solution and 0.05% Tween 80 aqueous solution were employed as the dissolution media. The dissolution profiles in the two media of the freeze-dried Amoitone B nanocrystals (NC-Am), the physical mixture, and pure Amoitone B were shown in Fig. 8. Since Pluronic F68 and lecithin are surfactants which have the effects of solubilization, emulsification and wetting, they might be the reasons for increasing the dissolution rate of the physical mixture and NC-Am. As seen in Fig. 8(A), more than 90% of the drug was dissolved in 0.1% SDS solution for NC-Am after 1 h, while the dissolution of Amoitone B and physical mixture were only about 17.4% and 38.1% after the same time period. The similar dissolution behavior was also displayed in Fig. 8(B). The cumulative release percentage of NC-Am in 0.05% Tween solution had reached 95.0% after 2 h with Amoitone B and its physical mixture of just about 43.0% and 58.6%, respectively. According to the above results, we found that the nanocrystals could markedly improve the dissolution rate of Amoitone B, while the solubilization effect of the surfactants were limited.

As we know, drug dissolution takes place in two continuous processes, firstly, the drug dissolves from the surface of the particles to form saturated layer, then the drug molecules pass through the diffusion layer formed between the saturation layer and bulk solution, entering into the bulk solution under convection. The rate and extent of drug dissolution which were usually determined by the diffusion process could be described by the Noyes–Whitney equation: $dc/dt = D \times A \times (C_s - C_t)/h$ (Dressman et al., 1998). In the equation, dc/dt means dissolution velocity, D is the diffusion coefficient, A is the surface area, h is the diffusion distance, C_s is the saturation solubility, and C_t is the bulk concentration. According to the above equation, an increase in the surface area due to the reduction of particle size and the increased saturation solubility were the reasons for the prominently enhanced dissolution rate of nanocrystals. In addition, the diffusion distance h which is a part of the hydrodynamic boundary layer h_H can influence the dissolution velocity and is strongly dependent on the particle size. The reduced particle size of nanocrystals led to a decreased diffusion distance h and consequently an increased dissolution velocity, which could be explained by the Prandtl equation (Mosharraf and Nystrom, 1995). This equation is described by $h_H = k(L^{1/2}/V^{1/2})$, where h_H means the hydrodynamic boundary layer thickness, k denotes a constant, L is the length of the particle surface, and V is the relative velocity of the flowing liquid surrounding the particle. In conclusion, the increased dissolution effect of NC-Am was primarily attributed to the enlarged surface area, the increased saturation solubility and the decreased diffusion distance as a result of particle size reduction rather than the influences of the crystalline form and excipients.

3.8. Pharmacokinetic studies

The Amoitone B blood concentration–time curves after intravenous administration of NC-Am and Amoitone B solution in rabbits were shown in Fig. 9. The results indicated that Amoitone B solution was quickly removed from the circulating systems, but on the contrary, NC-Am exhibited a markedly delayed blood clearance. It was reported that the uptake of nanoparticles by reticulate endothelial system (RES) organs following intravenous injection might take a few minutes or hours, depending on particle size and composition. NC-Am with a mean particle size of 275.4 nm showed

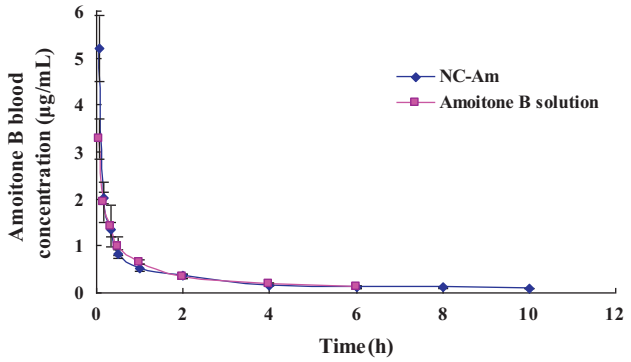

Fig. 9. The mean blood concentration–time curves of Amoitone B in rabbits following i.v. administration of NC-Am and Amoitone B solution at a dose of 8.0 mg kg^{-1}. Data were given as mean ± S.D., $n = 4$.

Table 3
Mean pharmacokinetic parameters of Amoitone B after administration of NC-Am and Amoitone B solution (each data was from four rabbits).

Parameter	Unit	NC-Am	Amoitone B solution
$AUC_{(0-\infty)}$	mg L^{-1} h)	4.902[a]	3.439
$t_{1/2\alpha}$	h	0.047	0.053
$t_{1/2\beta}$	h	0.67	0.436
$t_{1/2\gamma}$	h	8.446[a]	2.999
$MRT_{(0-\infty)}$	h	3.703[a]	2.257
CL	L/h/kg	1.632[a]	2.327
$V1$	L/kg	0.626[a]	0.283

[a] $P < 0.05$, statistical significance compared with Amoitone B solution group.

a rapid dissolution behavior and a higher Amoitone B concentration in blood circulation at the initial time point, but at the same time, it could be recognized and phagocytized by RES in blood circulation, primarily the macrophages in liver, spleen and lung (Gao et al., 2010; Liu et al., 2012b). The NC-Am uptaken by RES might dissolve in phagocytic cell and release slowly into blood circulation, thus maintaining a longer blood level compared to Amoitone B solution. The Amoitone B concentration–time curves for NC-Am and Amoitone B solution were fitted with the three-compartment model, and the main pharmacokinetic parameters were summarized in Table 3. Amoitone B in NC-Am was eliminated rather slowly with a larger $t_{1/2\gamma}$ (8.446 h) compared with Amoitone B solution (2.999 h). The AUC of NC-Am was larger than Amoitone B solution and there was a significant difference ($P < 0.05$) between them. We could deduce that NC-Am could improve the poor pharmacokinetic characteristics of Amoitone B by prolonging drug retention in vivo. Moreover, the aqueous preparation of Amoitone B which avoided systemic exposure to the organic solvent could be more acceptable for injection and remarkably reduce side effects, thus having an important clinical significance.

4. Conclusions

In this study, the Amoitone B nanocrystals with a homogeneous system were successfully prepared by the microfluidization method which was shown to be a simple and efficient technique for particle size reduction. In order to obtain the optimized nanosuspensions with small and uniform particle size, a narrow distribution and good short-term stability, the compositions of formula and parameters of microfluidization process were systematically investigated. For long-term stability, the nanosuspensions were transformed into lyophilized powders with mean particle size of 275.4 nm. The DSC and XRD analysis showed that the crystalline form of Amoitone B was not changed during the process of preparation and lyophilization. The in vitro solubility and dissolution studies confirmed that formulating Amoitone B as nanocrystals could increase the saturation solubility and dissolution rate to a great extent. The pharmacokinetics study demonstrated that the nanocrystals (NC-Am) did increase the Amoitone B concentration in plasma, retarded its clearance and exhibited the magnified AUC in vivo compared with Amoitone B solution. In addition, Amoitone B is a new compound which has only a few reports on its synthesis and biological activity, while up to now no study has been carried out on its dosage form design. So this paper is the first report on the pharmaceutical preparation for Amoitone B and may provide references for the development of injection and other preparations. In conclusion, developing Amoitone B as nanocrystals could not only solve the problem of insolubility but also reduce its side effects, and is expected to be a promising choice for intravenous delivery and further application to cancer therapy. Moreover, to further research the passive targeting characters and tumor inhibitory effects of Amoitone B nanocrystals, the tissue distribution and cytology experiments are in progress.

Acknowledgment

This work was supported by the National Basic Research Program of China (973Program), No. 2009CB930300.

References

Böhm, B.H., Müller, R.H., 1999. Lab-scale production unit design for nanosuspensions of sparingly soluble cytotoxic drugs. Pharm. Sci. Technol. Today 2, 336–339.
Bonta, P.I., Pols, T.W., de Vries, C.J., 2007. NR4A nuclear receptors in atherosclerosis and vein-graft disease. Trends Cardiovasc. Med. 17, 105–111.
Brady, S.F., Wagenaar, M.M., Singh, M.P., Janso, J.E., Clardy, J., 2000. The cytosporones, new octaketide antibiotics isolated from an endophytic fungus. Org. Lett. 2, 4043–4046.
Cerdeira, A.M., Mazzotti, M., Gander, B., 2010. Miconazole nanosuspensions: influence of formulation variables on particle size reduction and physical stability. Int. J. Pharm. 396, 210–218.
Chan, B.C., Ching, A.K., To, K.F., Leung, J.C., Chen, S., Li, Q., Lai, P.B., Tang, N.L., Shaw, P.C., Chan, J.Y., James, A.E., Lai, K.N., Lim, P.L., Lee, K.K., Chui, Y.L., 2008. BRE is an antiapoptotic protein in vivo and overexpressed in human hepatocellular carcinoma. Oncogene 27, 1208–1217.
Chen, H.B., Wan, J.L., Wang, Y.R., Mou, D.S., Liu, H.B., Xu, H.B., Yang, X.L., 2008. A facile nanoaggregation strategy for oral delivery of hydrophobic drugs by utilizing acid–base neutralization reactions. Nanotechnology 19, 375104.
Chen, H.B., Khemtong, C., Yang, X.L., Chang, X.L., Gao, J.M., 2011. Nanonization strategies for poorly water-soluble drugs. Drug Discov. Today 16, 354–360.
Chen, J.F., Zhou, M.Y., Shao, L., Wang, Y.Y., Yun, J., Chew, N.Y., Chan, H.K., 2004. Feasibility of preparing nanodrugs by high-gravity reactive precipitation. Int. J. Pharm. 269, 267–274.
Cho, S.D., Yoon, K., Chintharlapalli, S., Abdelrahim, M., Lei, P., Hamilton, S., Khan, S., Ramaiah, S.K., Safe, S., 2007. Nur77 agonists induce proapoptotic genes and responses in colon cancer cells through nuclear receptor-dependent and nuclear receptor-independent pathways. Cancer Res. 67, 674–683.
Dolenc, A., Kristl, J., Baumgartner, S., Planinsek, O., 2009. Advantages of celecoxib nanosuspension formulation and transformation into tablets. Int. J. Pharm. 376, 204–212.
Dressman, J.B., Amidon, G.L., Shah, V.P., Reppas, C., 1998. Dissolution testing as a prognostic tool for oral drug absorption: immediate release dosage forms. Pharm. Res. 15, 11–22.
Fakes, M.G., Vakkalagadda, B.J., Qian, F., Desikan, S., Gandhi, R.B., Lai, C., Hsieh, A., Franchini, M.K., Toale, H., Brown, J., 2009. Enhancement of oral bioavailability of an HIV-attachment inhibitor by nanosizing and amorphous formulation approaches. Int. J. Pharm. 370, 167–174.
Gao, L., Zhang, D.R., Chen, M.H., 2008a. Drug nanocrystals for the formulation of poorly soluble drugs and its application as a potential drug delivery system. J. Nanopart. Res. 10, 845–862.
Gao, L., Zhang, D.R., Chen, M.H., Duan, C.X., Dai, W.T., Jia, L.J., Zhao, W.F., 2008b. Studies on pharmacokinetics and tissue distribution of oridonin nanosuspensions. Int. J. Pharm. 355, 321–327.
Gao, Y., Li, Z.G., Sun, M., Li, H.L., Guo, C.Y., Cui, J., Li, A.G., Cao, F.L., Xi, Y.W., Lou, H.X., Zhai, G.X., 2010. Preparation, characterization, pharmacokinetics, and tissue distribution of curcumin nanosuspension with TPGS as stabilizer. Drug Dev. Ind. Pharm. 36, 1225–1234.
Kayser, O., 2001. A new approach for targeting to *Cryptosporidium parvum* using mucoadhesive nanosuspensions: research and applications. Int. J. Pharm. 214, 83–85.
Keck, C.M., Muller, R.H., 2006. Drug nanocrystals of poorly soluble drugs produced by high pressure homogenisation. Eur. J. Pharm. Biopharm. 62, 3–16.

Kolluri, S.K., Bruey-Sedano, N., Cao, X., Lin, B., Lin, F., Han, Y.-H., Dawson, M.I., Zhang, X.K., 2003. Mitogenic effect of orphan receptor TR3 and its regulation by MEKK1 in lung cancer cells. Mol. Cell. Biol. 23, 8651–8667.

Latha, S., Selvamani, P., Kumar, C.S., Sharavanan, P., Suganya, G., Beniwal, V.S., Rao, P.R., 2009. Formulation development and evaluation of metronidazole magnetic nanosuspension as a magnetic-targeted and polymeric-controlled drug delivery system. J. Magn. Magn. Mater. 321, 1580–1585.

Li, Q., Ching, A.K., Chan, B.C., Chow, S.K., Lim, P.L., Ho, T.C., Ip, W.K., Wong, C.K., Lam, C.W., Lee, K.K., Chan, J.Y., Chui, Y.L., 2004. A death receptor-associated anti-apoptotic protein, BRE, inhibits mitochondrial apoptotic pathway. J. Biol. Chem. 279, 52106–52116.

Li, Q.-X., Ke, N., Sundaram, R., Wong-Staal, F., 2006. NR4A1, 2, 3 – an orphan nuclear hormone receptor family involved in cell apoptosis and carcinogenesis. Histol. Histopathol. 21, 533–540.

Lin, B.Z., Kolluri, S.K., Lin, F., Liu, W., Han, Y.H., Cao, X.H., Dawson, M.I., Reed, J.C., Zhang, X.K., 2004. Conversion of Bcl-2 from protector to killer by interaction with nuclear orphan receptor Nur77/TR3. Cell 116, 527–540.

Liu, J.J., Zeng, H.N., Zhang, L.R., Zhan, Y.Y., Chen, Y., Wang, Y., Wang, J., Xiang, S.H., Liu, W.J., Wang, W.J., Chen, H.Z., Shen, Y.M., Su, W.J., Huang, P.Q., Zhang, H.K., Wu, Q., 2010. A unique pharmacophore for activation of the nuclear orphan receptor Nur77 in vivo and in vitro. Cancer Res. 70, 3628–3637.

Liu, Y., Xie, P.C., Zhang, D.R., Zhang, Q., 2012a. A mini review of nanosuspensions development. J. Drug Target. 20, 209–223.

Liu, Y., Zhang, D.R., Duan, C.X., Jia, L.J., Xie, P.C., Zheng, D.D., Wang, F.H., Liu, G.P., Hao, L.L., Zhang, X.S., Zhang, Q., 2012b. Studies on pharmacokinetics and tissue distribution of bifendate nanosuspensions for intravenous delivery. J. Microencapsul. 29, 194–203.

Maruyama, K., Tsukada, T., Ohkura, N., Bandoh, S., Hosono, T., Yamaguchi, K., 1998. The NGFI-B subfamily of the nuclear receptor superfamily. Int. J. Oncol. 12, 1237–1243 (Review).

Moll, U.M., Marchenko, N., Zhang, X.-K., 2006. P53 and Nur77/TR3 – transcription factors that directly target mitochondria for cell death induction. Oncogene 25, 4725–4743.

Mosharraf, M., Nystrom, C., 1995. The effect of particle size and shape on the surface specific dissolution rate of micronized practically insoluble drugs. Int. J. Pharm. 122, 35–47.

Mou, D.S., Chen, H.B., Wan, J.L., Xu, H.B., Yang, X.L., 2011. Potent dried drug nanosuspensions for oral bioavailability enhancement of poorly soluble drugs with pH-dependent solubility. Int. J. Pharm. 413, 237–244.

Muller, R.H., Keck, C.M., 2004. Challenges and solutions for the delivery of biotech drugs—a review of drug nanocrystal technology and lipid nanoparticles. J. Biotechnol. 113, 151–170.

Pei, L.M., Waki, H., Vaitheesvaran, B., Wilpitz, D.C., Kurland, I.J., Tontonoz, P., 2006. NR4A orphan nuclear receptors are transcriptional regulators of hepatic glucose metabolism. Nat. Med. 12, 1048–1055.

Sibayama-Imazu, T., Fujisawa, Y., Masuda, Y., Aiuchi, T., Nakajo, S., Itabe, H., Nakaya, K., 2008. Induction of apoptosis in PA-1 ovarian cancer cells by vitamin K_2 is associated with an increase in the level of TR3/Nur77 and its accumulation in mitochondria and nuclei. J. Cancer Res. Clin. Oncol. 134, 803–812.

Thassu, D., Deleers, M., Pathak, Y., 2007. Nanoparticulate Drug Delivery Systems. Informa Healthcare, New York.

Thompson, J., Winoto, A., 2008. During negative selection, Nur77 family proteins translocate to mitochondria where they associate with Bcl-2 and expose its proapoptotic BH3 domain. J. Exp. Med. 205, 1029–1036.

Tsai, M.L., Tseng, L.Z., Chen, R.H., 2009. Two-stage microfluidization combined with ultrafiltration treatment for chitosan mass production and molecular weight manipulation. Carbohydr. Polym. 77, 767–772.

Verma, S., Lan, Y., Gokhale, R., Burgess, D.J., 2009a. Quality by design approach to understand the process of nanosuspension preparation. Int. J. Pharm. 377, 185–198.

Verma, S., Gokhale, R., Burgess, D.J., 2009b. A comparative study of top-down and bottom-up approaches for the preparation of micro/nanosuspensions. Int. J. Pharm. 380, 216–222.

Wang, Y.C., Zhang, D.R., Liu, Z.P., Liu, G.P., Duan, C.X., Jia, L.J., Feng, F.F., Zhang, X.Y., Shi, Y.Q., Zhang, Q., 2010. In vitro and in vivo evaluation of silybin nanosuspensions for oral and intravenous delivery. Nanotechnology 21, 155104.

Winoto, A., Littman, D.R., 2002. Nuclear hormone receptors in T lymphocytes. Cell 109 (Suppl.), S57–S66.

Wu, Q., Liu, S., Ye, X.F., Huang, Z.W., Su, W.J., 2002. Dual roles of Nur77 in selective regulation of apoptosis and cell cycle by TPA and ATRA in gastric cancer cell. Carcinogenesis 23, 1583–1592.

Yoon, K., Lee, S.O., Cho, S.D., Kim, K., Khan, S., Safe, S., 2011. Activation of nuclear TR3 (NR4A1) by a diindolylmethane analog induces apoptosis and proapoptotic genes in pancreatic cancer cells and tumors. Carcinogenesis 32, 836–842.

Zhan, Y.Y., Du, X.P., Chen, H.Z., Liu, J.J., Zhao, B.X., Huang, D.H., Li, G.D., Xu, Q.Y., Zhang, M.Q., Weimer, B.C., Chen, D., Cheng, Z., Zhang, L.R., Li, Q.X., Li, S.W., Zheng, Z.H., Song, S.Y., Huang, Y.J., Ye, Z.Y., Su, W.J., Lin, S.C., Shen, Y.M., Wu, Q., 2008. Cytosporone B is an agonist for nuclear orphan receptor Nur77. Nat. Chem. Biol. 4, 548–556.

Zhang, T.C., Chen, J.N., Zhang, Y., Shen, Q., Pan, W.S., 2011. Characterization and evaluation of nanostructured lipid carrier as a vehicle for oral delivery of etoposide. Eur. J. Pharm. Sci. 43, 174–179.